PHYSICAL REVIEW C **69**, 031603(R) (2004)

Anomalous increase in width of fission fragment mass distribution in $^{19}F+^{232}Th$

T. K. Ghosh, S. Pal, T. Sinha, N. Majumdar, S. Chattopadhyay, and P. Bhattacharya
Saha Institute of Nuclear Physics, 1/AF Bidhan Nagar, Kolkata 700 064, India

A. Saxena and P. K. Sahu
Nuclear Physics Division, Bhabha Atomic Research Centre, Mumbai-400085, India

K. S. Golda and S. K. Datta
Nuclear Science Centre, New Delhi-110067, India

(Received 19 December 2003; published 18 March 2004)

Fission fragment mass distribution has been studied for the system $^{19}F+^{232}Th$ over an energy range of 105.4 MeV to 84.2 MeV in laboratory frame. For energies, above the Coulomb barrier, the variance of the mass distributions σ_m^2 varies linearly with temperature of the fused system, signifying statistical fusion-fission reaction. However, as energy decreases through the Coulomb barrier, a rapid increase in σ_m^2 is observed for the first time which may be a signal of onset of orientation dependent quasifission reaction.

DOI: 10.1103/PhysRevC.69.031603 PACS number(s): 25.70.Jj

In heavy ion induced fission reactions on heavy targets, anomalous enhancements of the fragment angular anisotropy with respect to the predictions of the statistical saddle point model (SSPM) [1] have been observed near and below the Coulomb barrier [2–4]. To explain enhancement in fragment anisotropy in near and sub barrier energies Hinde *et al.* [3] assumed an nuclear orientation dependent quasifission reaction wherein the dinuclear system before statistical equilibration moves over a mass asymmetric conditional saddle point, leading to a narrower K distribution compared to that expected from SSPM. Probable effects of the assumed quasifission process, apart from enhancement of fragment angular anisotropy, would be a asymmetry or increase in width of fission fragment mass distribution [5] and a suppression of the production cross section for evaporation residues in fusion reactions [6]. However, no strong dependence of the width of the fragment mass distribution or asymmetry in mass distribution was observed in $^{16}O+^{238}U$ [7]. The production of evaporation residues were found to be hindered by Berriman *et al.* [8] but this effect was not observed by Sonzogni *et al.* [9]. Vorkapic and Ivanisevic [10] suggested an alternate explanation of the observed anomalous angular distributions. They contended that, in subbarrier energies, fusion of projectile occurs only when the prolate deformed target is oriented in the beam direction, producing a narrow initial K distribution peaked around $K=0$. In their model, the K equilibration time was also assumed to be not too short compared to fission time. Using time dependent K distribution, a narrower K distribution compared to SSPM predictions could be envisaged and fragment angular anisotropy could be explained. However, in the above scenario, no abnormal behaviour in fission fragments mass distribution or yield of fusion evaporation residues was predicted.

In $^{19}F+^{232}Th$, a pronounced increase in angular anisotropy was observed [4] in near and subbarrier energies. In this communication, we report precise measurements of fragment mass distributions in $^{19}F+^{232}Th$ reaction from above to below Coulomb barrier energies, in the energy range 105.4–84.2 MeV. Fission fragment mass distribution from the fully equilibrated compound nucleus of $^{19}F+^{232}Th$ is expected to be decided at the scission point due to a long descent from saddle to scission [11]. Since shell effects are expected to be washed out at these excitations, the mass distributions should be symmetric with a smooth increase in width of the distribution with temperature. Any sudden change in the width of the mass distribution would indicate departure from full equilibration, while onset of mass asymmetry or a sudden increase in width of mass distribution would be a strong signal of quasifission.

The experiment was carried out using pulsed ^{19}F beam from the 15UD Pelletron at the Nuclear Science Centre (NSC), New Delhi. The pulse width was about 1.5 ns with a pulse separation of 250 ns. The target was a self-supporting 1.8 mg/cm^2 foil of ^{232}Th. The average center of mass energies cited include correction for energy loss in the target. The target was placed at an angle 30° to the beam. Fission fragments were detected with two large area X-Y position sensitive multiwire proportional counters (MWPCs) [12,13]. These detectors provide good timing and position resolution and can discriminate the fission fragments from beamlike particles. The active area of the detectors were 24 cm $\times$10 cm and were positioned at 65° and 95° to the beam respectively. The detectors were placed at 52.6 and 33.2 cm from the target, subtending polar (azimuthal) angles of 25°(±5°) and 39°(±8.5°), respectively. The operating pressure was maintained at about 3.0 torr of isobutane gas. The polar angle of emitted fission fragments could be determined with accuracy better than 0.2° while the accuracy in azimuthal angle was about 0.8°. Two solid state detectors were placed at ±10° with respect to the beam to detect elastically scattered ^{19}F particles to monitor beam intensity and positioning of beam on target. One of the solid-state detectors was also used for monitoring of the time structure of the beam. Time structure of the beam was also monitored intermittently by measuring the width of pulse with a fast plastic scintillator.

For each fission event, the time difference of the fast anode pulses of the detectors with respect to the pulsed beam,

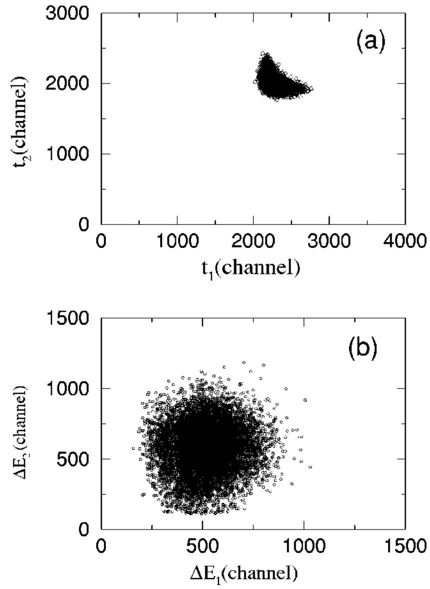

FIG. 1. The (a) time and (b) energy loss correlations of simultaneously detected fission fragments at $E_{\mathrm{cm}}=85.3$ MeV.

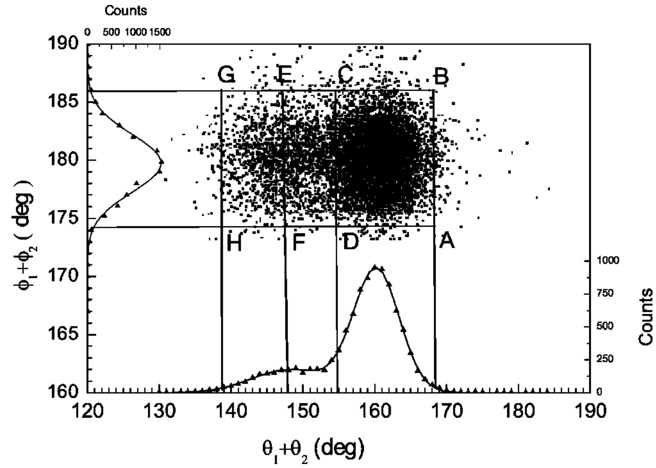

FIG. 2. Distributions of complimentary fission fragments in (θ,ϕ) at $E_{\mathrm{cm}}=85.3$ MeV. Rectangle ABCD indicates the gate used to select the fusion-fission events for mass determination. Rectangles ABEF and ABGH indicate the gate used to add 50% and 100 % of TF events, respectively.

the X and Y positions and the energy loss of fission fragments were measured. The trigger signal for the data acquisition system was generated by taking coincidence between any of the anode signals and the master oscillator of the pulsing system. The detection efficiency of fission fragments was better than 95% and the estimated mass resolution for fission fragments was about 3 a.m.u.

The masses of the fission fragments were determined event by event from precise measurements of flight paths and flight time differences of the complimentary fission fragments using the following set of equations [14]:

$$m_1 = \frac{(t_1 - t_2) + \delta t_0 + m_{\mathrm{CN}} d_2/p_2}{d_1/p_1 + d_2/p_2}, \tag{1}$$

$$m_2 = m_{\mathrm{CN}} - m_1, \tag{2}$$

$$p_1 = \frac{m_{\mathrm{CN}} V_{\mathrm{CN}}}{\cos\,\theta_1 + \sin\,\theta_1 \cot\,\theta_2}, \tag{3}$$

$$p_2 = \frac{p_1 \sin\,\theta_1}{\sin\,\theta_2}, \tag{4}$$

where m_1, m_2 are the fragment masses; t_1 and t_2 are the flight times of the fragments for the flight paths d_1 and d_2; p_1 and p_2 are the linear momenta of the fragments in laboratory frame; m_{CN} and V_{CN} are the mass and velocity of the compound nucleus. The difference in machine time for the two time of flight spectra δt_0 was determined precisely for each beam energy from the required identity of the measured mass distributions in two detectors.

The fission fragments were well separated from elastic and quasielastic channels, both in time and energy loss spectra. The time and energy loss correlations of the fission fragments which were detected simultaneously in the two detectors are shown in Fig. 1. The contributions of elastic and quasielastic channels were estimated to be less than 0.1% in these spectra.

The fission fragments from compound nuclear fission events were exclusively determined from the distributions of polar (θ) and azimuthal (ϕ) angles. The observed distributions of the complimentary fission events in (θ,ϕ) plane are shown in Fig. 2. The events enclosed by the rectangle ABCD in the figure are the fragments from fusion fission reaction. The projections on θ and ϕ planes are shown in the insets. At different energies, the window on the folding angles of fission fragments was varied to estimate the effect of any admixture of non compound fission channels. In Fig. 3 the measured variances of the fission mass distributions are shown as a function of the admixture of transfer followed by

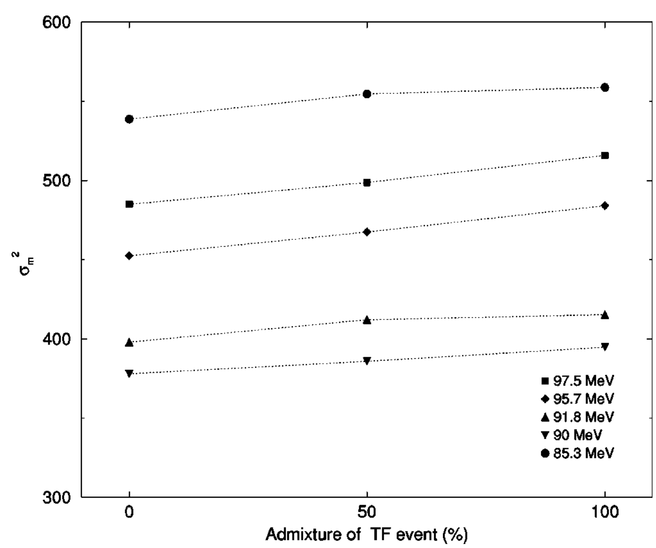

FIG. 3. Variance of mass distributions at different projectile energies (c.m.) as a function of admixture of transfer fission (TF) events. The dotted lines are guide to the eye.

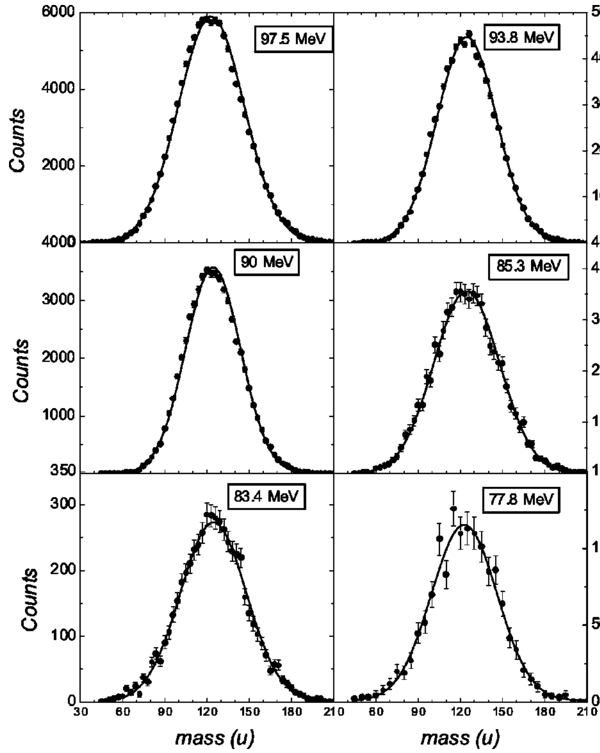

FIG. 4. Mass distributions at different projectile energies (c.m.). The Gaussian fits are shown by solid lines.

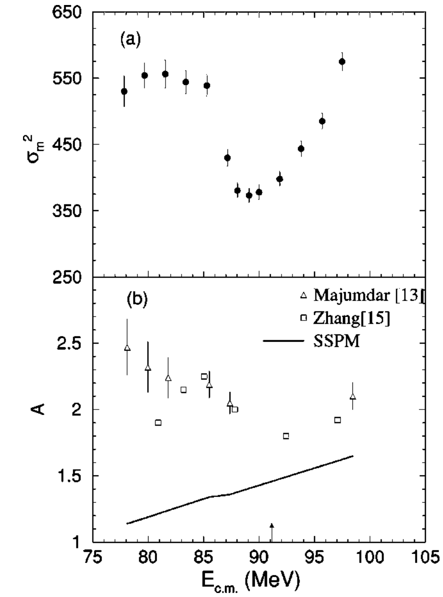

FIG. 5. (a) Mass variance σ_m^2 and (b) anisotropy A, as a function of E_{cm}. In (b) the solid line represent the SSPM calculation with correction for prescission neutron correction [13]. Coulomb barrier is indicated by an arrow.

fission (TF) events at different center-of-mass (c.m.) energies. The width of the distribution for any energy shows a slow increase (less than 10%) with admixture of TF events. Even at lower energies the contribution of TF events does not affect the mass distributions significantly.

A systematic study of the effects of different geometrical factors eliminated the systematic errors in determination of the polar and azimuthal angles for a precise measurement of the velocities of the fragments. The mass distributions at six representative c.m. energies, namely, 97.5, 93.8, 90, 85.3, 83.4, and 77.8 MeV are shown in Fig. 4. The mass distributions at all energies can be fitted with a single Gaussian (as shown by solid line), with peak close to the half of the combined target-projectile mass. We have not observed any significant admixture of an asymmetric mass distribution in the measured mass distributions.

The variation of the variances of the fitted Gaussians σ_m^2 to the experimental masses, as a function of the c.m. energies are shown in Fig. 5 (filled circles). Above the fusion barrier, σ_m^2 decreases with decrease in energy and the smooth linear variation with temperature shows that the fission is from a fully equilibrated compound nucleus. However, as the energy is decreased below the barrier, a sudden, almost 50% increase in the value of σ_m^2 is observed. With further decrease to subbarrier energies, σ_m^2 remains nearly constant with a small decreasing trend. However, these values are substantially larger than the value at the barrier. The slow and linear increase in σ_m^2 values with increasing admixture of TF events as shown in Fig. 3 clearly indicates that the observed variation in σ_m^2 with energy cannot be due to the admixture of TF events. It is to be noted that this variation of σ_m^2 is very similar to that observed trend of the angular anisotropy of the fission fragments (A), with energy. The variation of A with energy as observed by Majumdar *et al.* [13] and Zhang *et al.* [15] is shown in the lower panel of Fig. 5.

The sudden and large increase in the width of the mass distribution near the barrier signifies the onset of a completely different reaction mechanism other than statistical fusion-fission. This different reaction mechanism dominates the fission events at subbarrier energies. The definite correspondence of the change of the mass distribution widths with that of the average value of A at subbarrier energies, strongly support the assumption of quasifission reaction [3], where the dinuclear system passes over a conditional saddle point without equilibration in all degrees of freedom.

It is to be noted that this is the first observation of a rapid change of the width of fragment mass distribution with projectile energy and in fact, is a much stronger signal of onset of nonstatistical effects in $^{19}\mathrm{F}+{}^{232}\mathrm{Th}$ fusion fission reaction near barrier than the anomalous fission fragment angular anisotropy. It will be interesting to study this signal, i.e, the width of the mass distribution, on either side of Businaro-Gallone ridge of entrance channel mass asymmetry.

We are thankful to P. Barua and Professor S. Mukhopadhyay for their help during the experiment and the staff of NSC Pelletron for providing the good quality of beam required for the experiment.

[1] I. Halpern and V. M. Strutinsky, in *Proceeding of 2nd International Conference on Peaceful Uses of Atomic Energy*, Geneva (United Nations Publication, Geneva, 1958), Vol. 15, p. 408.
[2] V. S. Rammurthy and S. S. Kapoor, Phys. Rev. Lett. **54**, 178 (1985).
[3] D. J. Hinde *et al.*, Phys. Rev. Lett. **74**, 1295 (1995).
[4] N. Majumdar *et al.*, Phys. Rev. Lett. **77**, 5027 (1996).
[5] W. Q. Shen *et al.*, Phys. Rev. C **36**, 115 (1987).
[6] J. P. Blocki *et al.*, Nucl. Phys. A **459**, 145 (1986).
[7] D. J. Hinde *et al.*, Phys. Rev. C **53**, 1290 (1996).
[8] A. C. Berriman *et al.*, Nature (London) **413**, 144 (2001).
[9] A. A. Sonzogni *et al.*, Phys. Rev. C **58**, R1873 (1998).
[10] D. Vorkapic and B. Ivanisevic, Phys. Rev. C **52**, 1980 (1995).
[11] D. V. Vanin *et al.*, Phys. Rev. C **59**, 2114 (1999).
[12] P. Bhattacharya *et al.*, Nuovo Cimento Soc. Ital. Fis., A **108**, 819 (1995).
[13] N. Majumdar *et al.*, Phys. Rev. C **51**, 3109 (1995).
[14] R. K. Choudhury *et al.*, Phys. Rev. C **60**, 054609 (1999).
[15] H. Zhang *et al.*, Phys. Rev. C **49**, 926 (1994).